



axioms

IMPACT
FACTOR
1.6

Article

The Conservative Field of Coupled Newton–Coulomb Sources: Component Coupling Constants, Mass \rightleftharpoons Charge Cross-Forces, and Radiation from Reissner–Nordström Black Hole Mergers

Dimitris M. Christodoulou, Demosthenes Kazanas and Silas G. T. Laycock

Special Issue

Mathematical Aspects of Black Holes in General Relativity and Beyond

Edited by

Dr. Mehrab Momennia



<https://doi.org/10.3390/axioms14110845>

Article

The Conservative Field of Coupled Newton–Coulomb Sources: Component Coupling Constants, Mass \rightleftharpoons Charge Cross-Forces, and Radiation from Reissner–Nordström Black Hole Mergers

Dimitris M. Christodoulou ^{1,*} , Demosthenes Kazanas ²  and Silas G. T. Laycock ¹ 

¹ Lowell Center for Space Science and Technology, University of Massachusetts Lowell, Lowell, MA 01854, USA; silas_laycock@uml.edu

² Astrophysics Science Division, Code 663, NASA Goddard Space Flight Center, Greenbelt, MD 20771, USA; demos.kazanas@nasa.org

* Correspondence: dimitris_christodoulou@uml.edu or dchris32@depaul.edu

[†] Current address: Department of Mathematical Sciences, DePaul University, Chicago, IL 60614, USA.

Abstract

We investigate a combined conservative field, in which classical gravitational and electrostatic sources also exhibit mutual interactions. Hitherto neglected, the coupling between mass and charge may be necessary for constructing a unified conservative force field generated by a single underlying source. We determine the coupling constant of the cross-field components as the geometric mean (G-M) of Newton's G and Coulomb's K constants, in both SI units and dimensionless form. Consequently, for two identical objects, the cross-force (F_x) is the G-M of the familiar Newton (F_g) and Coulomb (F_e) forces, so that $F_x = \sqrt{F_g F_e}$, where $F_g \ll F_x \ll F_e$. Remarkably, such cross-forces should be measurable in torsion balance experiments involving a suspended neutral mass interacting with a partially ionized gas. Furthermore, we apply our new formulation to estimate the dimensionless amplitude $\|\mathcal{H}_{\alpha\beta}^{TT}\|$ of gravitational waves that are emitted by inspiraling Reissner–Nordström (RN) black hole binaries, expressed in terms of ratios of the four fundamental lengths of the problem: the distance to the binary D , the binary separation R , the Schwarzschild radius $R_S \propto 2M$ of mass M , and the RN charge (Q) length scale $L_Q \propto 2Q$. In this classical setting with speeds much lower than the speed of light c in vacuum, the surprising appearance of the maximum relativistic tension force $F_{\max} = c^4/(4G)$ is duly noted.

Keywords: black holes; cosmology; coupling constants; fine-structure constant; gravitation; gravitational waves; Planck units

MSC: 83-10; 83C35; 83C50; 83D05



Academic Editor: Mehrab Momennia

Received: 16 October 2025

Revised: 8 November 2025

Accepted: 12 November 2025

Published: 18 November 2025

Citation: Christodoulou, D.M.; Kazanas, D.; Laycock, S.G.T. The Conservative Field of Coupled Newton–Coulomb Sources: Component Coupling Constants, Mass \rightleftharpoons Charge Cross-Forces, and Radiation from Reissner–Nordström Black Hole Mergers. *Axioms* **2025**, *14*, 845. <https://doi.org/10.3390/axioms14110845>

Copyright: © 2025 by the authors. Licensee MDPI, Basel, Switzerland. This article is an open access article distributed under the terms and conditions of the Creative Commons Attribution (CC BY) license (<https://creativecommons.org/licenses/by/4.0/>).

1. Introduction

In a classical grand-unified framework, conservative long-range fields must arise from a single underlying principle governing the two fundamental properties known as inertial mass and static charge, along with their interactions with other fields. In such a setting, the field components themselves are expected to interact, much like those of the electromagnetic (EM) field. Yet the possibility of a coupling between mass and charge has largely been overlooked, since Coulomb's law and Newton's law of gravitation treat their sources independently.

Charges never exist in isolation; they are always bound to material objects. This strongly suggests that the conservative field inherently carries both sources together, making it difficult to conceive of them as acting entirely independently. In fact, one might even argue that a subtle form of blending is already encoded in these sources, since attraction of a test particle is a property shared by both mass and negative charge (their field lines are identical). Further corroborating evidence comes from the formal analogies between general relativity and classical electrodynamics that effectively describe the geometrical properties of spacetime by various sets of Maxwell equations for the ‘gravitational electric’ and ‘gravitational magnetic’ fields [1–4].

1.1. Principles of Source Coupling and Field Components

Here, we investigate the “GravElectroMagnetic” (GEM) forces that arise in a combined conservative long-range field, in which mass and charge are intrinsically coupled. The specific form of this coupling is carefully developed through a series of assumptions and procedures:

1. By convention, all attractive (repulsive) force components are taken to be positive (negative).
2. Coulomb’s law and Newton’s law of gravitation are the fundamental principles governing interactions between charges and masses, respectively. Symbolically, we write $F_{Q \rightarrow q}$, $F_{M \rightarrow m}$ for the actions and $F_{q \rightarrow Q}$, $F_{m \rightarrow M}$ for the reactions, respectively.
3. As usual, the coupling constants in the force laws are Coulomb’s constant K for charges and Newton’s gravitational constant G for masses. In dimensionless form, they appear in the definitions of the fine-structure constant (FSC) α_e and the gravitational coupling constant (GCC) α_g , respectively—but these definitions are written in terms of Planck’s constant h [5,6], not Dirac’s \hbar [7,8], and they are adopted as the new standard forms for the reasons explained in depth in Refs. [9,10].
4. The coupling constant of the cross-forces $F_{Q \rightarrow m}$, $F_{M \rightarrow q}$ and the corresponding reactions $F_{m \rightarrow Q}$, $F_{q \rightarrow M}$ is determined to be the geometric mean (G-M) \sqrt{GK} on dimensional grounds. A new, dimensionless, cross-coupling constant (CCC) α_{\times} then emerges, the G-M $\sqrt{\alpha_e \alpha_g}$, which is also defined in terms of Planck’s constant h , not Dirac’s \hbar . The coupling constants and the magnitudes of the various force components are summarized in Table 1.
5. Newton’s third law of action–reaction is assumed to remain valid in the presence of cross-forces. However, this assumption does not uniquely determine the signs of the cross-force components $Q \rightarrow m$, $M \rightarrow q$, or the corresponding reactions. There are two possibilities for mass–charge interactions: mass behaves either as a negative charge or as a positive charge. Consequently, a choice must be made on how the sources of the combined field should behave during mutual interactions, all the while obeying Newton’s third law of motion.
6. We assume that mass behaves as a negative charge in its interactions with charges, so that a test charge ($q = 1$) will be attracted by a mass M , and a test mass ($m = 1$) will be repelled by a negative charge Q (Figure 1). This choice is based on the similarity of the conventional force fields that are generated by a mass and a negative charge, where the radial field lines converge toward both of these sources (Figure 2). This assumption will have to be experimentally tested (see item 8 below).
7. Thus, $F_{+Q \rightarrow m}$, $F_{M \rightarrow +q}$ are attractive force components, and $F_{-Q \rightarrow m}$, $F_{M \rightarrow -q}$ are repulsive force components. The signs of the various force components are summarized in Table 2.
8. On the basis advocated above, we reject the notion that mass may behave as a positive charge in its interactions with charges of any type. However, Newton’s third law

of motion would be valid under this alternative hypothesis. The question of which hypothesis is right (or whether both of them are flawed) can be resolved by torsion balance experiments utilizing an electrically neutral mass interacting with a partially ionized gas.

Table 1. Coupling constants and magnitudes of the force components of the combined conservative field.

Pairwise Interaction	Force Constant	Force Magnitude	Coupling Constant	Definition (Using Planck's h)
$M \rightarrow m$	G	$(GM)m/R^2$	GCC	$\alpha_g = Gm_e^2/(hc)$
$Q \rightarrow q$	K	$(KQ)q/R^2$	FSC	$\alpha_e = Ke^2/(hc)$
$M \rightarrow q$	\sqrt{GK}	$(\sqrt{GKM})q/R^2$	CCC	$\alpha_x = \sqrt{\alpha_g \alpha_e}$
$Q \rightarrow m$	\sqrt{GK}	$(\sqrt{GKQ})m/R^2$	CCC	$\alpha_x = \sqrt{\alpha_g \alpha_e}$

Notes. G : Newton's constant; K : Coulomb's constant; m_e : Electron mass; e : Elementary charge; h : Planck's constant; c : Speed of light in vacuum [11]; R : Distance or separation of masses; α_e : Fine-structure constant (FSC) [12]; α_g : Gravitational coupling constant (GCC); α_x : Cross-coupling constant (CCC) [10]. All dimensionless coupling constants are defined in terms of Planck's h , not Dirac's \hbar . The parentheses in the magnitudes of the forces (column 3) highlight the source terms of the combined field.

Table 2. Attractive (+) and repulsive (−) conservative force components. The matrix is symmetric, so the reaction forces obey the same sign rules. There is no need for an equivalence principle of masses in this scheme: all masses are inertial, and they are rendered sources of gravity only when multiplied by Newton's G [10]. Similarly, charges scaled by Coulomb's K act as sources of electric fields.

		Subjected to Force		
		$+m$	$-q$	$+q$
Sources	$+M$	+	−	+
	$-Q$	−	−	+
	$+Q$	+	+	−

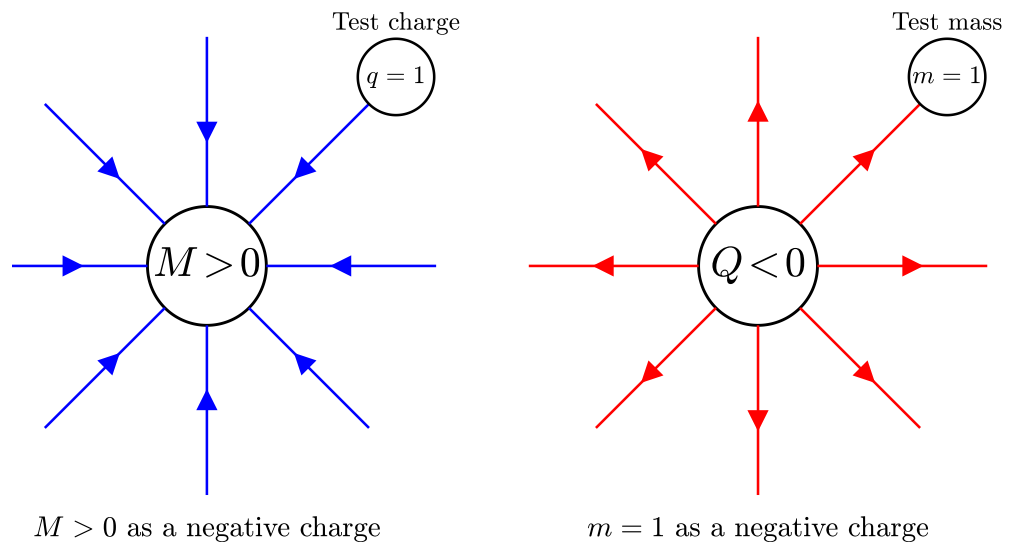


Figure 1. Cross-forces: The gravitational cross-field due to mass M (left panel) and the electrostatic cross-field due to negative charge Q (right panel). Masses M and m are assumed to behave as negative charges; thus, source M attracts the test charge $q = 1$, and source $Q < 0$ repels the test mass $m = 1$. On the other hand, a positive source Q (not depicted here) would attract the test mass $m = 1$, which behaves as a negative charge.

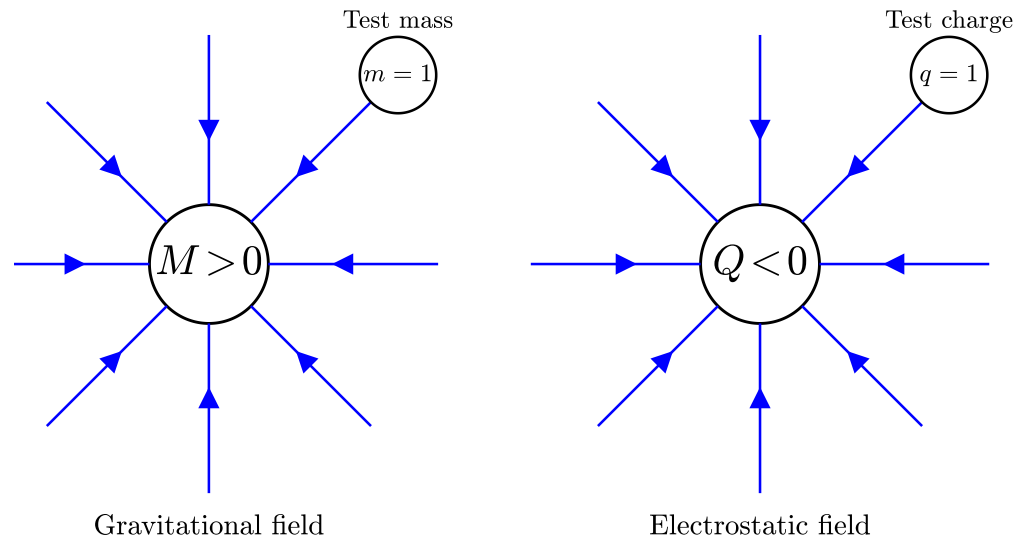


Figure 2. Newton’s law and Coulomb’s law: The gravitational field due to mass M (left panel) and the electrostatic field due to negative charge Q (right panel). The radial field lines converge toward both sources. The fields exhibit the same property: they attract test masses and test charges, respectively. On the other hand, a positive source Q (not depicted here) would repel the test charge $q = 1$ according to Coulomb’s law.

1.2. Outline

The remainder of the paper is organized as follows:

- In Section 2, we determine the coupling constant of the cross-forces acting between masses and charges and the conservative net forces of the interactions $(M, \pm Q) \rightarrow (m, \pm q)$, where capital letters denote the field sources, and lower-case letters denote the objects subjected to forcing.
- In Section 3, we estimate the magnitudes of the cross-forces between a neutral mass and an ionized xenon gas, with the prospect of measuring the effect in torsion balance experiments.
- In Section 4, we apply the new formulation to estimate the characteristic amplitude of radiation emitted by two inspiraling Reissner–Nordström (RN) black holes.
- In Section 5, we summarize our results and present our conclusions.

2. Newton–Coulomb Couplings, Cross-Forces, and Resultant GEM Forces

2.1. Dimensional Analysis of Cross-Forces and Effective Gravity

In general, we use capital letters to denote the sources M and Q of the conservative field and lower-case letters to indicate the masses (m) and the charges (q) that are subjected to cross-forces of the types $\{M \rightarrow q, Q \rightarrow m\}$. It can be shown that a cross-force law of the form $F \propto Mq/R^2$ or $F \propto Qm/R^2$ requires a proportionality constant with dimensions of $([G] \cdot [K])^{1/2}$. The dimensional analysis proceeds as follows:

$$\begin{aligned}
 [G] \cdot \frac{[M]^2}{[R]^2} \sim [F] \sim [K] \cdot \frac{[Q]^2}{[R]^2} &\Rightarrow [F] \cdot [F] \sim \left([G] \cdot \frac{[M]^2}{[R]^2}\right) \cdot \left([K] \cdot \frac{[Q]^2}{[R]^2}\right) \\
 &\Rightarrow [F]^2 \sim ([G] \cdot [K]) \cdot \left(\frac{[M]^2 [Q]^2}{[R]^4}\right) \tag{1} \\
 &\Rightarrow [F] \sim ([G] \cdot [K])^{1/2} \cdot \left(\frac{[M][Q]}{[R]^2}\right).
 \end{aligned}$$

Thus, the CCC that appears in both types of cross-forces is the $G\text{-}M\sqrt{GK}$ of Newton’s constant G and Coulomb’s constant K , irrespective of whether the source term involves

mass M acting on charge q or charge Q acting on mass m . The G-M \sqrt{GK} has been determined to 10 significant digits in SI units (Table C2 in Ref. [10]):

$$\sqrt{GK} = 0.774\,487\,2895 \text{ m}^3 \text{ s}^{-2} \text{ C}^{-1}. \tag{2}$$

The SI units in Equation (2) reveal the significance of this constant: Since $(\text{m}^3 \text{ s}^{-2})$ is the SI unit of the gravitational parameter GM (the source of gravity) [13,14], $[G] = (\text{m}^3 \text{ s}^{-2}) \text{ kg}^{-1}$ expresses the strength of this source per kilogram, and the G-M $[\sqrt{GK}] = (\text{m}^3 \text{ s}^{-2}) \text{ C}^{-1}$ expresses the strength of the same source per coulomb. The notion of an intrinsic coupling within the combined field is alluded to by these dimensional relations.

Furthermore, the other G-M of G and K , viz., $[\sqrt{G/K}] = \text{C kg}^{-1}$, leaves the source term out and directly describes coulombs per kilogram. This G-M guides us to define the effective gravitational constant G_\star [10] as

$$G_\star \equiv \frac{G}{K} = (4\pi\epsilon_0)G, \tag{3}$$

where $K = 1/(4\pi\epsilon_0)$, and ϵ_0 is the electric permittivity of the vacuum. The units of G_\star are $(\text{C kg}^{-1})^2$. Then, we also see that

$$[G_\star][M]^2 = [Q]^2, \tag{4}$$

which is a familiar relation between the units of mass and charge. In particular, $G_\star M_P^2 = Q_P^2$ in Planck (P) units and $G_\star M_S^2 = e^2$ in Stoney (S) units [10].

2.2. The Significance of the Effective Gravitational Constant G_\star

The G-M of Newton’s G and Coulomb’s K (Equation (2)) is the coupling constant of the cross-forces, so the postulated interaction between masses and charges does not introduce another universal constant. Nevertheless, it is rather odd that the combined GEM field is characterized by two seemingly independent constants, G and K . One would expect a single GEM constant, just as it was found for the electroweak field [9,10], in which the weak coupling constant α_w is related to the FSC α_e (defined in Table 1) by

$$\alpha_w = \sqrt{\alpha_e}. \tag{5}$$

This G - K relation puzzle is resolved in a unified GEM-weak field, where all three constants are related and the effective gravitational constant G_\star (Equation (3)) assumes a prominent role. The constants of the three fundamental forces are related by

$$\alpha_w = \frac{e}{Q_P} = \frac{e}{\sqrt{G_\star}M_P}, \tag{6}$$

where M_P is the Planck mass (defined in terms of Planck’s h) and Q_P is the Planck charge [10]. This relation is equivalent to

$$\alpha_w\sqrt{G_\star} = \frac{1}{N_A} \left(\frac{e}{m_e} \right), \tag{7}$$

where N_A is the “reduced Avogadro number” (reduced by a factor of ≈ 10 , as derived in Ref. [10]).

In Equation (7), the combination of constants G , K , and α_w (or the FSC α_e ; Equation (5)) collected on the left-hand side is expressed in terms of the properties of the electron (N_A is the number of electrons in ≈ 0.1 moles). This equation effectively relates $\sqrt{G_\star}$ to the ratio

(e/m_e) , a result that was expected on dimensional grounds, since both terms have SI units of $C\ kg^{-1}$. Thus, much like the electroweak constants α_e and α_w , the GEM constants G and K are not independent.

2.2.1. Numerical Equations for G_* and G

On the other hand, recent work has shown that Newton’s G can be obtained in a fundamentally different way—using strictly SI units—as follows:

First, we obtain G_* from the numerical equality (Equation (30) in Ref. [10])

$$\mathcal{N}(\sqrt{G_*}) = \frac{\mathcal{N}(k_B)}{\mathcal{N}(e)} \times 10^{-6}, \tag{8}$$

where the numerical function $\mathcal{N}(x)$ retains only the numerical value of x , and k_B is Boltzmann’s constant. This numerical relation indicates that entropy and charge information is encoded into G_* .

Next, we obtain Coulomb’s K from the electric permittivity of the vacuum ϵ_0 , viz.,

$$K \equiv \frac{1}{4\pi\epsilon_0}. \tag{9}$$

Finally, we combine Equations (8) and (9), and we solve for G . We determine that the numerical value of G in the SI system of units is

$$\mathcal{N}(G) = \frac{10^{-12}}{\mathcal{N}(4\pi\epsilon_0)} \left[\frac{\mathcal{N}(k_B)}{\mathcal{N}(e)} \right]^2 = 6.674\ 015\ 081 \times 10^{-11}, \tag{10}$$

a value that is precise to 10 significant digits [10] owing to the exceptional measurement precision of k_B , e , and ϵ_0 [11].

2.2.2. Remarks

It is worth noting that, although precise, the numerical equality (10) that produces the SI value of G is also the first instance in physics in which the term $(4\pi\epsilon_0)e^2$ appears as a product in the denominator of the fraction on the right-hand side.

Furthermore, since the vacuum permittivity ϵ_0 in the denominator is a lower limit in nature, it seems that the deduced SI value of G is a maximum in nature.

It is rather ironic that the extremely weak gravitational constant G , as we know it and have measured it, turns out to be a natural upper limit dictated by the vacuum, just as the speed of light in vacuum c . The difference of course is that c is a kinematical upper limit, whereas G is a maximized dynamical constant of the gravitational field.

2.3. The Components of the Conservative Force Field

Accounting explicitly for the signs of the force components given in Tables 1 and 2, we write the net forces F_{net} in the various cases as follows:

1. Source $(M, +Q) \rightarrow (m, +q)$: $F_{\text{net}} = |F|_{M \rightarrow m} + |F|_{M \rightarrow +q} + |F|_{+Q \rightarrow m} - |F|_{+Q \rightarrow +q}$.
2. Source $(M, -Q) \rightarrow (m, -q)$: $F_{\text{net}} = |F|_{M \rightarrow m} - |F|_{M \rightarrow -q} - |F|_{-Q \rightarrow m} - |F|_{-Q \rightarrow -q}$.
3. Source $(M, +Q) \rightarrow (m, -q)$: $F_{\text{net}} = |F|_{M \rightarrow m} - |F|_{M \rightarrow -q} + |F|_{+Q \rightarrow m} + |F|_{+Q \rightarrow -q}$.
4. Source $(M, -Q) \rightarrow (m, +q)$: $F_{\text{net}} = |F|_{M \rightarrow m} + |F|_{M \rightarrow +q} - |F|_{-Q \rightarrow m} + |F|_{-Q \rightarrow +q}$.

All four cases can be condensed into one equation, if the charges Q and q are allowed to carry their own signs implicitly. Then, we write the net force in the general form

$$\begin{aligned}
 F_{\text{net}} &= \left(\frac{1}{R^2}\right) \cdot [(GM + \sqrt{GK} Q) m - (KQ - \sqrt{GK} M) q] \\
 &= \left(\frac{K}{R^2}\right) \cdot [(G_* M + \sqrt{G_*} Q) m - (Q - \sqrt{G_*} M) q].
 \end{aligned}
 \tag{11}$$

or, equivalently, in the matrix form

$$\begin{aligned}
 F_{\text{net}} &= \left(\frac{1}{R^2}\right) \cdot [M \ Q] \begin{bmatrix} G & \sqrt{GK} \\ \sqrt{GK} & -K \end{bmatrix} \begin{bmatrix} m \\ q \end{bmatrix} \\
 &= \left(\frac{K}{R^2}\right) \cdot [M \ Q] \begin{bmatrix} G_* & \sqrt{G_*} \\ \sqrt{G_*} & -1 \end{bmatrix} \begin{bmatrix} m \\ q \end{bmatrix}.
 \end{aligned}
 \tag{12}$$

The 2×2 interaction matrix

$$\mathcal{J}_* = \begin{bmatrix} G_* & \sqrt{G_*} \\ \sqrt{G_*} & -1 \end{bmatrix},
 \tag{13}$$

is symmetric, i.e., identical to its transpose $(\mathcal{J}_*)^T$. Its eigenvalues (λ_e, λ_g) are real, and its eigenvectors (\vec{v}_e, \vec{v}_g) are orthogonal. These eigenvectors define independent normal modes of interaction. Since $G \ll K$, then $G_* \ll 1$, and the eigenvalues are $\lambda_e \approx -(1 + G_*)$ and $\lambda_g \approx 2G_*$ to the first order in G_* . The corresponding eigenvectors in this approximation are $\vec{v}_e \approx [\sqrt{G_*} \ -1]^T$ and $\vec{v}_g \approx [+1 \ \sqrt{G_*}]^T$.

In the physical regime where $G_* \ll 1$, the two normal modes are identified as predominantly electrical and gravitational, respectively. The off-diagonal components $\sim \sqrt{G_*}$ indicate that each mode is weakly coupled to the other interaction. The eigenvalues of the system then show that the electrical mode $\propto \exp(\lambda_e t)$ decays rapidly in time t at a rate of $\lambda_e \approx -1$, whereas the gravitational mode $\propto \exp(\lambda_g t)$ is nearly quasistatic and evolves very slowly at a rate of $\lambda_g \approx 2G_* \ll 1$. As a result, once the fast electrical mode has decayed, the long-term evolution of the system is governed primarily by the very slow gravitational interactions.

2.4. Dimensionless Coupling Constants and Forces Between Electrons

Applied to two interacting electrons of mass m_e and charge $-e < 0$, Equation (11) becomes

$$F_{\text{net}} = \frac{1}{R^2} (G m_e^2 - 2\sqrt{GK} e m_e - K e^2) \quad (\text{repulsive}),
 \tag{14}$$

where the dominant Coulomb force ($\propto -e^2$) and the two cross-forces ($\propto -em_e$) are all repulsive. The cross-force components cancel out only in a $e^+ \rightleftharpoons e^-$ interaction, for which $Qm + Mq = 0$ in Equation (11) and the net force $F_{\text{net}} \simeq +Ke^2/R^2$ is predominantly due to Coulomb attraction.

A dimensionless coupling constant of the combined field is defined for each component of the net force (14) in reference to the product (hc) , where h is Planck's constant and c is the speed of light in vacuum. Thus, we define the GCC, the CCC, and the FSC as

$$\alpha_g \equiv \frac{G m_e^2}{hc} = 2.787\ 972\ 231 \times 10^{-46},
 \tag{15}$$

$$\alpha_x \equiv \frac{\sqrt{G}K_e m_e}{hc} = 5.690\,323\,437 \times 10^{-25}, \tag{16}$$

and

$$\alpha_e \equiv \frac{Ke^2}{hc} = 1.161\,409\,732 \times 10^{-3} \simeq \frac{1}{861}, \tag{17}$$

respectively. The numerical values of these constants were determined from CODATA and PDG measurements [11,12] and the new data obtained in Refs. [9,10].

It is easy to show that the coupling constants are related, as they should be in the combined field: the CCC is precisely the G-M of the FSC and the GCC, viz.,

$$\alpha_x = \sqrt{\alpha_g \alpha_e}. \tag{18}$$

Thus, we see that the coupling constants $\{\alpha_g, \alpha_x, \alpha_e\}$ form a growing geometric progression, in which $\alpha_g \ll \alpha_x \ll \alpha_e$, and the common ratio $\sqrt{\alpha_e/\alpha_g} \simeq 2.04 \times 10^{21}$ represents the square root of the ratio (E_e/E_g) of the electrostatic to the gravitational potential energy of two electrons separated by any distance R .

As a result, the net force (14) between the two electrons can be written as

$$\begin{aligned} F_{\text{net}} &= \frac{hc}{R^2} \left(-\alpha_e - 2\sqrt{\alpha_g \alpha_e} + \alpha_g \right) \\ &= \frac{hc}{R^2} (-\alpha_e) (1 + 2\sqrt{\beta_g} - \beta_g) \\ &\simeq F_{\text{Coulomb}} (1 + 2\sqrt{\beta_g}) \quad (\text{repulsive}). \end{aligned} \tag{19}$$

where the normalized GCC $\beta_g \equiv \alpha_g/\alpha_e \simeq 2.40 \times 10^{-43}$ [10], and the term $-\beta_g$ was neglected in the last step.

Thus, the perturbation to the Coulomb force between electrons effectively arises from the cross-forces. Their relative amplitude ($2\sqrt{\beta_g} \sim 10^{-21}$) is many orders of magnitude larger than that of the purely gravitational component, which was neglected. This disparity raises the prospect of detecting the cross-forces (should they exist) in gravitational experiments that involve an ionized gas and a neutral mass. Some typical estimates are obtained in Section 3 below.

3. Action–Reaction Cross-Forces of Type $Q \rightleftharpoons m$ in Torsion Balance Experiments

Consider a partially ionized noble gas of mass M and total ionic charge Q interacting with a neutral mass m , located at distance R . For the interaction $(M, Q) \rightarrow (m, q)$ with $Q > 0$ and $q = 0$, Equation (11) reduces to

$$F_{\text{net}} = F_{\text{Newton}} \left(1 + \frac{Q}{\sqrt{G_*}M} \right) \quad (\text{attractive}), \tag{20}$$

where $F_{\text{Newton}} = GMm/R^2$, and G_* is given by Equation (3). The cross-term is positive and enhances the Newtonian force.

For a torsion balance setup, we choose a test mass of $m = 12$ g and a xenon ($_{54}\text{Xe}$) attractor with mass $M = 12$ g and a relatively small ionization fraction χ (to be determined). The $_{54}\text{Xe}$ attractor is pressurized to 10 atm at room temperature (300 K) to reduce its volume to easily manageable Lab levels. Under these conditions, the ideal gas law predicts a volume of $V = 225$ cm³ (0.225 L) for 0.0914 moles (12 g) of $_{54}\text{Xe}$ gas (standard atomic weight 131.293 g mol⁻¹ [15]).

The two masses are separated by a distance of $r = 12$ cm, so that the Newtonian force of attraction, $F_{\text{Newton}} = 6.67 \times 10^{-13}$ N, is barely measurable in the Lab. On the other

hand, we would like the cross-force to be easily measurable in the Lab, so we choose its magnitude to be $F_x = 1 \times 10^{-8}$ N, which implies that $Q/(\sqrt{G_*}M) = 1.50 \times 10^4$. Then, the required xenon charge is

$$Q = +15.5 \text{ nC}, \tag{21}$$

corresponding to a low ionization fraction of

$$\chi = \frac{Q/e}{N_{Xe}} = 1.76 \times 10^{-12}, \tag{22}$$

where $N_{Xe} = 5.50 \times 10^{22}$ is the total number of atoms in 12 grams of ^{54}Xe gas.

Finally, for a rod with a typical lever arm of $\ell = 2.5$ cm, the generated torque is

$$\tau = F_x \ell = 2.50 \times 10^{-10} \text{ Nm}, \tag{23}$$

and for a torsion constant of $k = 1 \times 10^{-9}$ N m rad⁻¹ (typical of Lab-utilized tungsten or quartz fibers), the maximum angular deflection of the suspended rod is

$$\theta_{\max} = \frac{\tau}{k} = 0.250 \text{ rad} = 14.3^\circ. \tag{24}$$

The above values fall within the operational range of modern torsion balance metrology (e.g., Refs. [16–24] and references therein); therefore, if cross-forces do exist, their effects should be detectable with current experimental techniques using Faraday cages to achieve electrostatic shielding of the equipment [25–30].

4. Radiation from Inspiring Reissner–Nordström Black Holes

4.1. Preliminaries

An RN black hole is characterized by two independent length scales corresponding to its physical properties, the field sources M and Q [31,32]: the Schwarzschild radius

$$R_S = \frac{2GM}{c^2}, \tag{25}$$

and the charge radius

$$R_Q = \frac{\sqrt{GK}|Q|}{c^2},$$

where c is the speed of light in vacuum. Acceptable R_Q values that prevent the appearance of naked singularities [33] fall in the range of

$$0 \leq R_Q \leq \frac{R_S}{2}.$$

For our purposes, we choose a different strategy: we define an alternative charge length scale L_Q that carries a factor of 2 in analogy with R_S , as well as the sign of the charge Q if one or both black holes of a binary carry a negative charge, viz.,

$$L_Q \equiv \frac{2\sqrt{GK}Q}{c^2}, \tag{26}$$

for which the acceptable range to avoid naked singularities now is

$$|L_Q| \leq R_S. \tag{27}$$

Then, by substituting Equations (25) and (26) into Equation (11), we write the conservative resultant force between equal-mass ($M = m$) RN black holes in three cases of interest (equal charges $q = Q$, opposite charges $q = -Q$, and one zero charge $q = 0$):

$$\begin{aligned}
 \text{Case 1, } Qq = +Q^2 : F_{\text{net}} &= F_{\text{max}} \left(R_S^2 - L_Q^2 + 2R_S L_Q \right) R^{-2}; \\
 \text{Case 2, } Qq = -Q^2 : F_{\text{net}} &= F_{\text{max}} \left(R_S^2 + L_Q^2 \right) R^{-2}; \\
 \text{Case 3, } q = 0 : F_{\text{net}} &= F_{\text{max}} \left(R_S^2 + R_S L_Q \right) R^{-2};
 \end{aligned}
 \tag{28}$$

where R is the separation of the black holes, and $F_{\text{max}} = c^4/(4G)$ is the maximum tension force established in general relativity [34–37] (notably, one-fourth of the Planck unit of force $F_P = c^4/G$ [10,38]). Furthermore, $L_Q < 0$ when even one of the black holes carries a negative charge.

4.1.1. Maximum Force F_{max}

The significance of the maximum tension force is that F_{max} has indeed appeared in our classical analysis of GEM forces. Up until now, it was commonly believed that a maximum force could not be obtained in Newtonian gravity [35], although it was found in some modified theories of gravity that are applicable to black hole binaries (e.g., Moffat, Brans–Dicke, and pure Lovelock theories [37]).

The “absence” of F_{max} from Newtonian mechanics was previously attributed in part to the absence of Planck’s constant h from the definition of the Planck force F_P [35]. We see that this conjecture is not confirmed: when we consider all force components of the combined GEM field, force F_{max} appears naturally as the leading factor of the net force. We expect that $R_S^2 + L_Q^2 < R^2$ (even for $R = 2R_S$, when the horizons of the black holes touch), which then implies that the classical net forces F_{net} in binaries containing Schwarzschild and/or RN black holes do obey the condition that

$$F_{\text{net}} < F_{\text{max}} = \frac{c^4}{4G}.
 \tag{29}$$

4.1.2. Net Forces F_{net} in Cases 1–3

The net forces (28) can be further simplified by introducing the dimensionless ratio ϕ between the source terms of the combined GEM field, defined as

$$\phi \equiv \frac{L_Q}{R_S} = \frac{Q}{\sqrt{G_*}M},
 \tag{30}$$

where $\phi < 0$ when at least one of the black holes in a binary carries a negative charge. Under these conditions, Equation (28) can be rewritten as

$$\begin{aligned}
 \text{Case 1, } Qq = +Q^2 : F_{\text{net}} &= F_{\text{max}} \left(1 - \phi^2 + 2\phi \right) \left(R_S/R \right)^2; \\
 \text{Case 2, } Qq = -Q^2 : F_{\text{net}} &= F_{\text{max}} \left(1 + \phi^2 \right) \left(R_S/R \right)^2; \\
 \text{Case 3, } q = 0 : F_{\text{net}} &= F_{\text{max}} \left(1 + \phi \right) \left(R_S/R \right)^2.
 \end{aligned}
 \tag{31}$$

Now, interpreting Cases 2 and 3 is straightforward, but Case 1 presents additional subtleties:

- In Case 3, the ratio $\phi \in [-1, +1]$, and the surviving component of the cross-force (term $+\phi$) is repulsive only if $Q < 0$.

- In Case 2, the ratio $\phi \in [-1, +1]$ as well; the Coulomb force is attractive (term $+\phi^2$), and the cross-forces vanish.
- In Case 1, when $\phi < 1 - \sqrt{2}$, the net force is repulsive and the black holes move apart. Models involving two negatively charged black holes with $\phi < 1 - \sqrt{2}$ are not of interest, since the emitted GEM waves die out rapidly (their amplitudes decrease with separation as $1/R$ [39–41]). Such models are therefore excluded from the subsequent analysis of Case 1 by adopting the restricted range

$$1 - \sqrt{2} \leq \phi \leq 1 \quad (\text{Case 1}). \tag{32}$$

which corresponds to non-repulsive net forces $F_{\text{net}} \geq 0$.

4.2. Radiation Amplitudes

In linearized gravity, the typical amplitude A of the perturbation of the flat spacetime metric $\eta_{\alpha\beta}$ (i.e., the “metric perturbation” $h_{\alpha\beta}^{\text{TT}}$ with $A \equiv \|h_{\alpha\beta}^{\text{TT}}\| \ll 1$) is estimated to be (pages 996–1000 in Ref. [39] and Equations (4.38)–(4.40) in Ref. [40]) of the order of

$$A = \frac{G}{c^4} \left(\frac{2}{D} \right) \left| \frac{d^2}{dt^2} (I_{\text{RN}}) \right| = \frac{1}{F_{\text{P}}} \left(\frac{2}{D} \right) \left| \frac{d^2}{dt^2} (I_{\text{RN}}) \right|, \tag{33}$$

where t represents time, $I_{\text{RN}} = \mu R^2 = \frac{1}{2}MR^2$ is the moment of inertia of the RN binary (μ is the reduced mass), and D is the distance of the binary system from the observer.

We assume that the masses M of the black holes do not vary in time, in which case Equation (33) takes the equivalent forms

$$\begin{aligned} A &= \frac{1}{F_{\text{P}}} \left(\frac{M}{D} \right) \left| \frac{d^2}{dt^2} (R^2) \right| \\ &= \frac{2}{F_{\text{P}}} \left(\frac{R}{D} \right) \left| M \frac{d^2R}{dt^2} + \frac{M}{R} \left(\frac{dR}{dt} \right)^2 \right| \\ &= \frac{2}{F_{\text{P}}} \left(\frac{R}{D} \right) \left| -F_{\text{net}} + \frac{MV^2}{R} \right|; \end{aligned} \tag{34}$$

in these equations, the separation $R(t)$ is a decreasing function of time, the radial velocity is $V(t) = dR/dt < 0$, and the net force $F_{\text{net}} > 0$ is attractive (item 1 in Section 1.1).

Next, we adopt the equality $MV^2/R = F_{\text{net}}/3$, and we cast Equation (34) in a compact form, viz.,

$$A = \frac{4}{3} \left(\frac{R}{D} \right) \frac{F_{\text{net}}}{F_{\text{P}}} = \frac{1}{3} \left(\frac{R}{D} \right) \frac{F_{\text{net}}}{F_{\text{max}}}. \tag{35}$$

The relation $MV^2/R = F_{\text{net}}/3$ follows from the autonomous differential equation

$$R R'' = -3(R')^2, \tag{36}$$

where primes denote derivatives with respect to time t and the acceleration $R'' < 0$ during the inspiral. The general solution describing orbital decay is $R(t) \propto (1 - t/\tau_c)^{1/4}$, where τ_c is the so-called “coalescence time”, defined by the condition that $R(\tau_c) = 0$ [41–44]. This solution effectively describes energy losses in the system: the power that is radiated away by GEM waves is precisely equal to the rate of decrease of the binary’s orbital energy [45–47].

4.2.1. Schwarzschild Black Holes

For conventional gravitational waves in the absence of Coulomb and cross-forces ($\phi = 0$), all three cases presented in Equation (31) reduce to the Schwarzschild attractive force

$$F_S = F_{\max} \left(\frac{R_S}{R} \right)^2. \tag{37}$$

Then, Equation (35) produces an estimate of the expected amplitude of gravitational waves A_S from a pair of Schwarzschild black holes (SBHs), viz.,

$$A_S = \frac{R_S^2}{3RD}. \tag{38}$$

When the horizons of two SBHs touch, $R = 2R_S$ and $A_S = R_S/(6D)$. As an example, for $M = 5M_\odot$, $D = 8$ kpc, and horizons touching, the wave amplitude is quite large, viz., $A_S \simeq 1 \times 10^{-17}$. But for a binary separation of $R = 1$ pc at the same distance D , Equation (38) gives $A_S \simeq 1 \times 10^{-29}$, a signal that is weaker by 12 orders of magnitude.

4.2.2. Reissner–Nordström Black Holes

In general, the three cases presented in Equation (31), combined with Equation (35), yield the following GEM wave amplitudes for the corresponding ϕ -ranges that characterize RN black hole inspirals:

$$\begin{aligned} \text{Case 1, } Qq = +Q^2 : A &= A_S(1 - \phi^2 + 2\phi), \quad \text{for } (1 - \sqrt{2}) \leq \phi \leq 1; \\ \text{Case 2, } Qq = -Q^2 : A &= A_S(1 + \phi^2), \quad \text{for } -1 \leq \phi \leq 1; \\ \text{Case 3, } q = 0 : A &= A_S(1 + \phi), \quad \text{for } -1 \leq \phi \leq 1; \end{aligned} \tag{39}$$

where A_S is given by Equation (38).

In these cases, RN pairs of “extremal black holes” (EBHs) with $|\phi| = 1$ are of special interest [48,49]. Their GEM wave amplitudes are

$$A_{\text{EBHs}} = \begin{cases} 0 & , \text{ for } Q < 0 \text{ and } q = 0; \\ 2A_S & , \text{ in all the other cases.} \end{cases} \tag{40}$$

The corresponding extremal net forces, derived from Equations (31) and (37), are as follows:

$$F_{\text{EBHs}} = \begin{cases} 0 & , \text{ for } Q < 0 \text{ and } q = 0; \\ 2F_S & , \text{ in all the other cases.} \end{cases} \tag{41}$$

Extremal black hole binaries with $Q < 0$ and $q = 0$ constitute one of two new classes of stationary equilibria arising solely from the inclusion of cross-forces. The second class emerges in Case 1 for $Q = q = (1 - \sqrt{2})\sqrt{G_*}M$ (i.e., $\phi = 1 - \sqrt{2} < 0$). These equilibria are discussed further in Section 4.3 below.

4.3. GEM Radiation, Extremal Black Holes, and Two Classes of Stationary Equilibria

In the nominal case of gravitational radiation from black hole mergers, a pair of SBHs are subject to an attractive force $F_S > 0$ (Equation (37)), and the emitted gravitational waves have a typical amplitude A_S , given by Equation (38).

Considering now Equations (39)–(41), the following types of black hole binaries (RN–RN and RN–SBH pairs) are of current theoretical interest:

- (a) RN black hole mergers with negligible charges ($|\phi| \ll 1$) are also effectively described by the nominal SBH mergers. However, the first-order approximations of $\mathcal{O}(\phi)$ are different in Cases 1–3: the slopes of the linear terms in Equation (39) are 2, 0, and 1, respectively.
- (b) Case 1: Black holes with the same mass M and the same negative charge $Q = (1 - \sqrt{2})\sqrt{G_*}M$ are in stationary equilibrium ($F_{\text{net}} = 0$ and $A = 0$). These models are discussed in more detail below.
- (c) Case 3: An RN black hole with a charge-to-mass ratio of $Q/M = -\sqrt{G_*} = -86.173\ 333\ \text{pC / kg}$ (i.e., $\phi = -1$) is also in stationary equilibrium, with an SBH of mass $m = M$ ($F_{\text{net}} = 0$), and no gravitational or GEM waves are emitted by the pair ($A = 0$). This equilibrium is established by the balance between the attractive Newtonian forces $M \rightleftharpoons m$ and the repulsive cross-forces $Q \rightleftharpoons m$, since $Q < 0$.
- (d) All other pairs of EBHs of equal mass M and at least one positive charge Q (Equations (40) and (41)) are bound by an attractive net force of magnitude $F_{\text{EBHs}} = 2F_S$ and emit GEM waves of amplitude $A_{\text{EBHs}} = 2A_S$, which grows at twice the rate of conventional gravitational waves during the inspiral.

4.3.1. Majumdar–Papapetrou RN–RN Binaries

The famous relativistic Majumdar–Papapetrou stationary equilibrium solution [50,51] is not realized in the above cases because of the inclusion of cross-forces. This equilibrium was originally established in extremal RN black holes of equal mass M and equal charge $Q = \pm\sqrt{G_*}M$ (hence, $|\phi| = 1$), in which the Newtonian gravitational attraction cancels exactly the Coulomb repulsion [52–55]. However, there exists an analogue of the Majumdar–Papapetrou model, in which $m = M$ and $Qq = +Q^2 \neq 0$ (a Case 1 model in Equation (39); item (b) above): For equal masses and charges, the net force is

$$F_{\text{net}} = F_S (1 - \phi^2 + 2\phi), \tag{42}$$

and a stationary equilibrium does arise for

$$\phi \equiv \phi_{\text{eq}} = 1 - \sqrt{2} \simeq -0.4142, \tag{43}$$

corresponding to a ratio of $Q/M \simeq -35.694\ 163\ \text{pC / kg}$. Naturally, no GEM waves are emitted from this RN–RN configuration ($A = 0$ from Equation (39) with $\phi = \phi_{\text{eq}}$ in Case 1).

4.3.2. Extremal RN–RN Binaries

Equation (40) shows that extremal RN–RN GEM waves are twice as strong and carry four times the energy flux of SBH–SBH gravitational waves (item (d) above). However, extremal RN black holes have not been observed, and only recently has it been shown that such objects can form through gravitational collapse [49,56]. These developments motivate a renewed examination of such models. For instance, a $5M_\odot$ RN black hole would require a charge excess or deficit of roughly 10^{16} moles of electrons ($|Q| \sim 10^{21}\ \text{C}$), corresponding to an ionization fraction of only $\sim 10^{-18}$, since five solar masses contain about 10^{34} moles of hydrogen atoms. For further details on the theoretically expected charge range in RN black holes and the limiting value of $\phi \equiv L_Q/R_S = \pm 1$ for extremal Majumdar–Papapetrou solutions, see Refs. [57–59], the online summaries [48,60,61], and the recent works [49,56,62–64].

5. Summary and Conclusions

In this work, we have investigated the conservative GEM fields generated by charged masses (M, Q) interacting with other charged masses (m, q). The appearance of force components due to cross-interactions between masses and charges ($M \rightleftharpoons q$ and $Q \rightleftharpoons m$) is the key new element introduced in the calculations. The steps taken in the analysis and the empirical results obtained from applications are summarized as follows:

1. The adopted principles of source coupling and the new and old GEM/EM forces were described in Section 1.1 and in Table 1. These principles are experimentally testable (Section 3).
2. Newton’s third law of motion holds for all resultant forces, but the mass in cross-terms was assumed to behave in analogy to a negative charge (Table 2), because both masses and negative charges invariably attract test particles with positive intrinsic properties. This assumption can also be tested experimentally (Section 3).
3. The dimensional coupling constant of the cross-forces was determined in Section 2.1 as the G-M of Newton’s G and Coulomb’s K (Equation (2)), and the resulting net forces due to both masses and charges were determined in Section 2.3 (Equations (11) and (12)).
4. The dimensionless coupling constants corresponding to Newton’s law of gravity, Coulomb’s law, and the new cross-force components were defined in Section 2.4 (Equations (15)–(17) and Table 1) using the dimensional constants of the classical force laws, properties of the electron (e, m_e), Planck’s constant h (not Dirac’s \hbar [9,10]), and the speed of light c .
5. The cross-force (F_x) between identical objects is the G-M of the familiar Newton (F_g) and Coulomb (F_e) forces, so that $F_g \ll F_x \ll F_e$. If present, these cross-forces should be measurable in torsion balance experiments involving suspended masses interacting with partially ionized gases. As an application of the new formulation, we obtained related estimates for setting up such experiments in Section 3.
6. In another application, we determined in Section 4 the typical amplitude $A = \|\hat{h}_{\alpha\beta}^{\text{TT}}\|$ of GEM waves from extremal RN–RN black holes of the same mass and charge magnitude. It was found that $A = 2A_S$, where A_S is the amplitude of gravitational waves from a pair of inspiraling Schwarzschild black holes (see Equations (37) and (38) for SBH–SBH binaries).
7. In the classical treatment of GEM forces in black hole binaries (Section 4), it is striking that the maximum relativistic tension force $F_{\text{max}} = c^4/(4G)$ emerges naturally (Equation (28)), even though this limit was discovered in relativistic calculations and was not anticipated to appear in a classical framework [34,35].
8. Because of the inclusion of cross-forces, the relativistic Majumdar–Papapetrou [50,51] stationary solution for extremal RN black holes ($\phi = \pm 1$ in Equation (30) and $Q/M \simeq \pm 86.17 \text{ pC / kg}$) shifts to a unique lower (non-extremal) negative charge value, viz., $\phi = 1 - \sqrt{2} \simeq -0.4142$ and $Q/M \simeq -35.69 \text{ pC / kg}$ (Section 4.3). This threshold serves as a separatrix: in our models, identical RN black holes with a ϕ -ratio in the negative range of

$$-1 \leq \phi < 1 - \sqrt{2},$$

do repel one another, whereas there are no repelling RN–RN or RN–SBH pairs in the absence of cross-forces.

9. The cross-forces in RN–SBH binaries with $M = m$ are also responsible for the emergence of another class of stationary nonradiating equilibria (item (c) in Section 4.3). In this class, the RN black hole is always extremal and negatively charged ($\phi = -1$), with a charge-to-mass ratio of $Q/M \simeq -86.17 \text{ pC / kg}$.

Author Contributions: Conceptualization, D.M.C. and D.K.; methodology, D.M.C. and S.G.T.L.; formal analysis, D.M.C.; investigation, D.M.C., D.K., and S.G.T.L.; resources, D.K. and S.G.T.L.; writing—original draft preparation, D.M.C.; writing—review and editing, D.K. and S.G.T.L.; project administration, D.K.; funding acquisition, S.G.T.L. All authors have read and agreed to the published version of the manuscript.

Funding: D.M.C. and S.G.T.L. acknowledge support from NSF-AAG grant No. AST-2109004.

Data Availability Statement: The original contributions presented in this study are included in the article. Further inquiries can be directed to the corresponding author.

Acknowledgments: We thank the reviewers of this paper for constructive comments and suggestions that have led to improvements of the presentation. Support from NASA, NSF, and LoCSST over the years is gratefully acknowledged by the authors.

Conflicts of Interest: The authors declare no conflict of interest.

Abbreviations

The following abbreviations are used in this manuscript:

CCC	Cross-Coupling Constant
CODATA	Committee On Data
EBH	Extremal Black Hole
EM	Electromagnetic
FSC	Fine-Structure Constant
GCC	Gravitational Coupling Constant
GEM	GravElectroMagnetic
G-M	Geometric Mean
Lab	Laboratory
PDG	Particle Data Group
RN	Reissner–Nordström
SBH	Schwarzschild Black Hole
SI	Système International d’unités
T	Transpose
TT	Transverse–Traceless

References

1. Boyeneni, S.; Wu, J.; Most, E.R. Unveiling the electrodynamic nature of spacetime collisions. *Phys. Rev. Lett.* **2025**, *135*, 101401. [CrossRef] [PubMed]
2. Olivares, H.; Peshkov, I.M.; Most, E.R.; Guercilena, F.M.; Papenfort, L.J. New first-order formulation of the Einstein equations exploiting analogies with electrodynamics. *Phys. Rev. D* **2022**, *105*, 124038. [CrossRef]
3. Ciufolini, I.; Wheeler, J.A. *Gravitation and Inertia*; Princeton University Press: Princeton, NJ, USA, 1995.
4. Gravitoelectromagnetism. Wikipedia. 2025. Available online: <https://en.wikipedia.org/wiki/Gravitoelectromagnetism> (accessed on 4 October 2025).
5. Planck, M. About irreversible radiation processes. In *Sitzungsberichte der Preussischen Akademie der Wissenschaften*; Verlag der akademie der wissenschaften: Berlin, Germany, 1899; p. 440.
6. Planck, M. Ueber irreversible Strahlungsvorgänge. *Ann. Phys.* **1900**, *4*, S.69. [CrossRef]
7. Dirac, P.A.M. On the theory of quantum mechanics. *Proc. R. Soc. Lond. A* **1926**, *112*, 661.
8. Dirac, P.A.M. *The Principles of Quantum Mechanics*; Oxford University Press: London, UK, 1930; p. 87.
9. Christodoulou, D.M.; Kazanas, D. The upgraded Planck system of units that reaches from the known Planck scale all the way down to subatomic scales. *Astronomy* **2023**, *2*, 235–268. [CrossRef]
10. Christodoulou, D.M.; Kazanas, D.; Laycock, S.G.T. Natural constants determined to high precision from Boltzmann’s constant and Avogadro’s number—A challenge to experiments and astrophysical observations to match the precision of the results. *Galaxies* **2025**, *13*, 119. [CrossRef]
11. Mohr, P.J.; Newell, D.B.; Taylor, B.N.; Tiesinga, E. CODATA recommended values of the fundamental physical constants: 2022. *Rev. Mod. Phys.* **2025**, *97*, 025002. [CrossRef]

12. Navas, S.; Amsler, C.; Gutsche, T.; Hanhart, C.; Hernández-Rey, J.J.; Lourenço, C.; Masoni, A.; Mikhasenko, M.; Anderson, J.; Zheng, W.; et al. Review of particle physics. *Phys. Rev. D* **2024**, *110*, 030001. [[CrossRef](#)]
13. Danby, J.M.A. *Fundamentals of Celestial Mechanics*, 2nd ed.; Willmann-Bell: Richmond, VA, USA, 1992; pp. 63+74.
14. Jacobson, R.A. The orbits of the main Saturnian satellites, the Saturnian system gravity field, and the orientation of Saturn's pole. *Astron. J.* **2022**, *164*, 199. [[CrossRef](#)]
15. Prohaska, T.; Irrgeher, J.; Benefield, J.; Böhlke, J.K.; Chesson, L.A.; Coplen, T.B.; Ding, T.; Dunn, P.J.H.; Gröning, M.; Holden, N.E. Standard atomic weights of the elements 2021 (IUPAC Technical Report). *Pure Appl. Chem.* **2022**, *94*, 573. [[CrossRef](#)]
16. Gundlach, J.H.; Merkowitz, S.M. Measurement of Newton's constant using a torsion balance with angular acceleration feedback. *Phys. Rev. Lett.* **2000**, *85*, 2869. [[CrossRef](#)] [[PubMed](#)]
17. Tu, L.C.; Luo, J.; Gillies, G.T. The measurement of the Newtonian gravitational constant. *Rep. Prog. Phys.* **2005**, *68*, 77. [[CrossRef](#)]
18. Kapner, D.J.; Cook, T.S.; Adelberger, E.G.; Gundlach, J.H.; Heckel, B.R.; Hoyle, C.D.; Swanson, H.E. Tests of the gravitational inverse-square law below the dark-energy length scale. *Phys. Rev. Lett.* **2007**, *98*, 021101. [[CrossRef](#)]
19. Schlamminger, S.; Choi, K.-Y.; Wagner, T.A.; Gundlach, J.H.; Adelberger, E.G. Test of the equivalence principle using a rotating torsion balance. *Phys. Rev. Lett.* **2008**, *100*, 041101. [[CrossRef](#)]
20. Schlamminger, S.; Gundlach, J.H.; Newman, R.D. Recent measurements of the gravitational constant as a function of time. *Phys. Rev. D* **2015**, *91*, 121101. [[CrossRef](#)]
21. Liu, D.; Peng, K.; He, Y. Direct measurement of torsional properties of single fibers. *Meas. Sci. Technol.* **2016**, *27*, 115017. [[CrossRef](#)]
22. Li, Q.; Xue, C.; Liu, J.-P.; Wu, J.-F.; Yang, S.-Q.; Shao, C.-G.; Quan, L.-D.; Tan, W.-H.; Tu, L.-C.; Liu, Q.; et al. Measurements of the gravitational constant using two independent methods. *Nature* **2018**, *560*, 582. [[CrossRef](#)]
23. Xue, C.; Liu, J.-P.; Li, Q.; Wu, J.-F.; Yang, S.-Q.; Liu, Q.; Shao, C.-G.; Tu, L.-C.; Hu, Z.-K.; Luo, J.; et al. Precision measurement of the Newtonian gravitational constant. *Natl. Sci. Rev.* **2020**, *7*, 1803. [[CrossRef](#)]
24. Wang, S.; Wang, Z.; Liu, D.; Dong, P.; Min, J.; Luo, Z.; Qi, K.; Lei, J. Torsion pendulum apparatus for ground testing of space inertial sensor. *Sensors* **2024**, *24*, 7816. [[CrossRef](#)] [[PubMed](#)]
25. Antonucci, F.; Cavalleri, A.; Dolesi, R.; Hueller, M.; Nicolodi, D.; Tu, H.B.; Vitale, S.; Weber, W.J. Interaction between stray electrostatic fields and a charged free-falling test mass. *Phys. Rev. Lett.* **2012**, *108*, 181101. [[CrossRef](#)] [[PubMed](#)]
26. Hewett, D.P.; Hewett, I.J. Correction to 'Homogenized boundary conditions and resonance effects in Faraday cages'. *Proc. R. Soc. A* **2017**, *473*, 20170331. [[CrossRef](#)]
27. Rothleitner, C.; Schlamminger, S. Invited Review Article: Measurements of the Newtonian constant of gravitation, G. *Rev. Sci. Instrum.* **2017**, *88*, 111101. [[CrossRef](#)]
28. Schlamminger, S.; Chao, L.S.; Lee, V.; Newell, D.B.; Speake, C.C. Design of an electrostatic feedback for an experiment to measure G. *IEEE Open J. Instrum. Meas.* **2022**, *1*, 1–10. [[CrossRef](#)]
29. Ke, J.; Dong, W.-C.; Huang, S.-H.; Tan, Y.-J.; Tan, W.-H.; Yang, S.-Q.; Shao, C.-G.; Luo, J. Electrostatic effect due to patch potentials between closely spaced surfaces. *Phys. Rev. D* **2023**, *107*, 065009. [[CrossRef](#)]
30. Song, C.; Hu, M.; Li, K.; Luo, P.-s.; Wang, S.; Yin, H.; Zhou, Z. A high precision surface potential imaging torsion pendulum facility to investigate physical mechanism of patch effect. *Rev. Sci. Instrum.* **2023**, *94*, 024501. [[CrossRef](#)] [[PubMed](#)]
31. Mahajan, S.M.; Qadir, A.; Valanju, V.M. Reintroducing the concept of «force» into relativity theory. *Nuovo Cim.* **1981**, *65*, 404. [[CrossRef](#)]
32. Qadir, A. Reissner-Nordstrom repulsion. *Phys. Lett. A* **1983**, *99*, 419. [[CrossRef](#)]
33. Reissner-Nordström Metric. Wikipedia. 2025. Available online: https://en.wikipedia.org/wiki/Reissner%E2%80%93Nordstr%C3%B6m_metric (accessed on 29 September 2025).
34. Gibbons, G.W. The maximum tension principle in general relativity. *Found. Phys.* **2002**, *32*, 1891. [[CrossRef](#)]
35. Barrow, J.D.; Gibbons, G.W. Maximum tension: With and without a cosmological constant. *Mon. Not. R. Astr. Soc.* **2015**, *446*, 3874. [[CrossRef](#)]
36. Barrow, J.D.; Gibbons, G.W. Maximum magnetic moment to angular momentum conjecture. *Phys. Rev. D* **2017**, *95*, 064040. [[CrossRef](#)]
37. Barrow, J.D.; Dadhich, N. Maximum force in modified gravity theories. *Phys. Rev. D* **2020**, *102*, 064018. [[CrossRef](#)]
38. Elert, G. The Physics Hypertextbook. 2025. Available online: <https://physics.info/planck/> (accessed on 29 September 2025).
39. Misner, C.W.; Thorne, K.S.; Wheeler, J.A. Evaluation of the Radiation Field in the Slow-Motion Approximation. In *Gravitation*; Freeman & Company: San Francisco, CA, USA, 1973; Chapter 36.10, pp. 996–1000.
40. Flanagan, É.É.; Hughes, S.A. The basics of gravitational wave theory. *New J. Phys.* **2005**, *7*, 204. [[CrossRef](#)]
41. Thorne, K.S. Multipole expansions of gravitational radiation. *Rev. Mod. Phys.* **1980**, *52*, 299. [[CrossRef](#)]
42. Cutler, C.; Flanagan, É.E. Gravitational waves from merging compact binaries: How accurately can one extract the binary's parameters from the inspiral waveform? *Phys. Rev. D* **1994**, *49*, 2658. [[CrossRef](#)]
43. Blanchet, L. Post-Newtonian theory for gravitational waves. *Living Rev. Relativ.* **2024**, *27*, 4. [[CrossRef](#)]

44. Dyadina, P. Gravitational waveforms from inspiral compact binaries in Hybrid metric-Palatini gravity. *Eur. Phys. J. C* **2025**, *85*, 643. [CrossRef]
45. Arun, K.G.; Iyer, B.R.; Qusailah, M.S.S.; Sathyaprakash, B.S. Testing post-Newtonian theory with gravitational wave observations. *Class. Quantum Grav.* **2006**, *23*, L37. [CrossRef]
46. Buonanno, A.; Iyer, B.R.; Ochsner, E.; Pan, Y.; Sathyaprakash, B.S. Comparison of post-Newtonian templates for compact binary inspiral signals in gravitational-wave detectors. *Phys. Rev. D* **2009**, *80*, 084043. [CrossRef]
47. Shiralilou, B.; Hinderer, T.; Nissanke, S.M.; Ortiz, N.; Witek, H. Post-Newtonian gravitational and scalar waves in scalar-Gauss–Bonnet gravity. *Class. Quantum Grav.* **2022**, *39*, 035002. [CrossRef]
48. Extremal Black Hole. Wikipedia. 2025. Available online: https://en.wikipedia.org/wiki/Extremal_black_hole (accessed on 4 October 2025).
49. Kehle, C.; Unger, R. Extremal black hole formation as a critical phenomenon. *arXiv* **2024**, arXiv:2402.10190. [CrossRef]
50. Majumdar, S.D. A class of exact solutions of Einstein’s field equations. *Phys. Rev.* **1947**, *72*, 390. [CrossRef]
51. Papapetrou, A. A static solution of the equations of the gravitational field for an arbitrary charge-distribution. *Proc. R. Ir. Acad.* **1947**, *A51*, 191.
52. Israel, W.; Wilson, G.A. A class of stationary electromagnetic vacuum fields. *J. Math. Phys.* **1972**, *13*, 865. [CrossRef]
53. Hartle, J.B.; Hawking, S.W. Solutions of the Einstein-Maxwell equations with many black holes. *Commun. Math. Phys.* **1972**, *26*, 87. [CrossRef]
54. Heusler, M. On the uniqueness of the Papapetrou-Majumdar metric. *Class. Quantum Grav.* **1997**, *14*, L129. [CrossRef]
55. Albacete, E.; Richartz, M. Tidal forces in Majumdar-Papapetrou spacetimes. *Universe* **2024**, *10*, 62. [CrossRef]
56. Kehle, C.; Unger, R. Gravitational collapse to extremal black holes and the third law of black hole thermodynamics. *J. Eur. Math. Soc.* **2025**, published online first. Available online: <https://ems.press/journals/jems/articles/14298531> (accessed on 5 October 2025).
57. Carter, B. Global structure of the Kerr family of gravitational fields. *Phys. Rev.* **1968**, *174*, 1559. [CrossRef]
58. Misner, C.W.; Thorne, K.S.; Wheeler, J.A. “Infinity” in Asymptotically Flat Spacetime. In *Gravitation*; Freeman & Company: San Francisco, CA, USA, 1973; Chapter 34.2, Exercise 34.3, pp. 920–921.
59. Kallosh, R.; Linde, A.; Ortin, T.; Peet, A.; Van Proeyen, A. Supersymmetry as a cosmic sensor. *Phys. Rev. D* **1992**, *46*, 5278. [CrossRef] [PubMed]
60. Wikipedia 2025, Black Hole. Available online: https://en.wikipedia.org/wiki/Black_hole (accessed on 29 September 2025).
61. Nadis, S. Mathematicians Prove Hawking Wrong About the Most Extreme Black Holes. *Quanta Magazine* **2024**. Available online: <https://www.quantamagazine.org/mathematicians-prove-hawking-wrong-about-extremal-black-holes-20240821> (accessed on 5 October 2025).
62. Carroll, S.M.; Johnson, M.C.; Randall, L. Extremal limits and black hole entropy. *J. High Energy Phys.* **2009**, *11*, 109. [CrossRef]
63. Kehle, C.; Unger, R. Event horizon gluing and black hole formation in vacuum: The very slowly rotating case. *Adv. Math.* **2024**, *452*, 109816. [CrossRef]
64. Di Filippo, F.; Liberati, S.; Visser, M. Fully extremal black holes: A black hole graveyard? *Int. J. Mod. Phys. D* **2024**, *33*, 2440005. [CrossRef]

Disclaimer/Publisher’s Note: The statements, opinions and data contained in all publications are solely those of the individual author(s) and contributor(s) and not of MDPI and/or the editor(s). MDPI and/or the editor(s) disclaim responsibility for any injury to people or property resulting from any ideas, methods, instructions or products referred to in the content.